Prognostic significance of p62/SQSTM1 subcellular localization and LC3B in oral squamous cell carcinoma

J-L Liu[1,2], F-F Chen[3], J Lung[4], C-H Lo[5], F-H Lee[5], Y-C Lu[6] and C-H Hung*,[2]

[1]Department of Pathology, St. Martin De Porres Hospital, No. 565, Sector 2, Daya Road, Chiayi City 600, Taiwan; [2]Graduate Institute of Clinical Medical Sciences, College of Medicine, Chang Gung University, No. 259, Wenhua 1st Road, Guishan Township, Taoyuan County 333, Taiwan; [3]Department of Pathology, Chang Gung Memorial Hospital at Chiayi, No. 6, W. Sector, Jiapu Road, Puzi City, Chiayi County 613, Taiwan; [4]Division of Pulmonary and Critical Care Medicine, Chang Gung Memorial Hospital at Chiayi, No. 6, W. Sector, Jiapu Road, Puzi City, Chiayi County 613, Taiwan; [5]Department of Oral and Maxillofacial Surgery, St. Martin De Porres Hospital, No. 565, Sector 2, Daya Road, Chiayi City 600, Taiwan and [6]Department of Otolaryngology, St. Martin De Porres Hospital, No. 565, Sector 2, Daya Road, Chiayi City 600, Taiwan

Background: Autophagy is a programmed cell survival mechanism that has a key role in both physiologic and pathologic conditions. The relationship between autophagy and cancer is complex because autophagy can act as either a tumour suppressor or as a tumour promoter. The role of autophagy in oral squamous cell carcinoma (OSCC) is controversial. Several studies have claimed that either a high or low expression of autophagy-related proteins was associated with poor prognosis of OSCCs. The aims of the study were to compare autophagy in OSCCs, verrucous hyperplasias, and normal oral mucosas, and to inspect the prognostic role of autophagy in OSCCs.

Methods: We used the autophagosome marker, LC3B, and autophagy flux marker, p62/SQSTM1 (p62), by using immunohistochemistry, and examined p62 mRNA by RNA *in situ* hybridization, to evaluate autophagy in 195 OSCCs, 47 verrucous hyperplasias, and 37 normal oral mucosas. The prognostic roles of LC3B and p62 protein expressions in OSCCs were investigated.

Results: We discovered that the normal oral mucosa exhibited limited LC3B punctae and weak cytoplasmic p62 staining, whereas the OSCCs exhibited a marked increase in LC3B punctae and cytoplasmic p62 expression. The expression pattern of LC3B and cytoplasmic p62 of the verrucous hyperplasias were between normal oral mucosas and OSCCs. The normal oral mucosas, verrucous hyperplasias, and OSCCs presented no differences in nuclear p62 expression and the p62 mRNA level. p62 mRNA expression was elevated in a minority of cases. High p62 mRNA expression was associated with high p62 protein expression in the cytoplasm. Increased LC3B punctae, high cytoplasmic p62, and low nuclear p62 expressions in OSCCs were associated with aggressive clinicopathologic features and unfavourable prognosis. In addition, low nuclear p62 expression was an independent prognostic factor for overall and disease-specific survival rates. Furthermore, we disclosed that high cytoplasmic p62 expression accompanied with either a low or high LC3B expression, which indicated autophagy impairment under basal or activated autophagic activity, was associated with aggressive behaviour in advanced OSCCs.

Conclusions: We suggested that autophagy was altered during cancer initiation and progression. Autophagy impairment contributed to cancer progression in advanced OSCCs.

Autophagy is a highly conserved programmed cell survival mechanism of eukaryotes. It is a dynamic process that consists of multiple steps to remove damaged intracellular proteins and organelles. The key double-membraned organelle, autophagosome, engulfs damaged intracellular contents and subsequently fuses with lysosomal membranes to form autolysosomes. Lysosomal enzymes degrade the engulfed contents of autolysosome to recycle the degraded molecules for cell survival (Mizushima, 2007). Autophagy is an essential physiological mechanism that maintains cellular homeostasis, particularly under stressful conditions (Kundu and Thompson, 2008). Recent evidence has suggested that a broad spectrum of diseases shows dysfunctional autophagy (Levine and Kroemer, 2008; Mizushima *et al*, 2008).

The role of autophagy in carcinogenesis is complex and not completely understood. Autophagy can act as a tumour suppressor by removing the damaged proteins and organelles, which may generate free radicals to cause genome instability (Shintani and Klionsky, 2004). An autophagy-related gene, *BECN1*, has been proven to be a haploinsufficient tumour suppressor (Qu *et al*, 2003; Yue *et al*, 2003). In addition, autophagy can promote cancer cell survival in an energy-deficient environment (Levine, 2007; Brech *et al*, 2009). The relationship between autophagy and the clinical outcomes of cancer patients is controversial. Clinical studies on various cancer types have observed that either low or high expression of autophagy-related proteins was linked to unfavourable prognosis (Huang *et al*, 2010; Koukourakis *et al*, 2010; Nicotra *et al*, 2010; Wan *et al*, 2010; Giatromanolaki *et al*, 2011a, b; Spowart *et al*, 2012; Won *et al*, 2012; Choi *et al*, 2013). The expression of autophagy-related proteins might be cell type-specific and stage-dependent.

Oral squamous cell carcinoma (OSCC) is the sixth most common cancer worldwide (Warnakulasuriya, 2009). Various studies have claimed that increase or decrease in autophagy-related proteins is associated with poor prognosis of OSCCs (Kapoor *et al*, 2012; Tang *et al*, 2013; Wang *et al*, 2013). In addition, autophagy-related protein expression in premalignant lesions and normal tissues has seldom been mentioned. In the present study, we used the autophagosome marker, LC3B, and autophagy flux marker, p62/SQSTM1 (p62) protein, as well as p62 mRNA, to examine autophagy in OSCCs, verrucous hyperplasias, and normal oral mucosas. We also investigated the prognostic significance of autophagy by examining LC3B and p62 expressions in OSCCs.

MATERIALS AND METHODS

Patients and tissue samples. This retrospective study was approved by the Institutional Review Board of St. Martin De Porres Hospital. We collected formalin-fixed, paraffin-embedded tissue blocks from surgical resected specimens of OSCC from the archives of St. Martin De Porres Hospital from January 2003 to December 2008. The inclusion criteria were tumour size ⩾5 mm and first diagnosed primary OSCC. Patients who received preoperative neoadjuvant therapy were excluded from this study. Clinical information and follow-up data were obtained from medical records. The tumour-node-metastasis stage was defined according to the seventh edition of the American Joint Committee on Cancer staging system. Overall survival was defined as the time between surgery and death of all causes. Disease-specific survival was defined as the time between surgery and death caused by OSCC. Recurrence-free survival was defined as the time between surgery and the first local or systemic recurrence.

Because of the field cancerisation of OSCC, we collected tissue blocks of normal oral mucosas and premalignant lesions independent from the cancer tissue. Oral mucosas from nonepithelial lesions, such as inflammation, lymphoid hyperplasia, or mucocele, were selected as the normal oral mucosas. Verrucous hyperplasias were selected as the premalignant lesions. Areas of cauterised artefact were avoided. Regarding the normal oral mucosas and verrucous hyperplasias, tissues containing oral mucosas larger than 5 mm were selected. Patients who presented with a history of OSCC before the surgery were excluded. Clinical information of age and sex of the patients were obtained from medical records.

Pathologic examination. The haematoxylin and eosin-stained slides of each case were reviewed and histologically confirmed by a pathologist. The histologic grade of the OSCC was classified as grade 1 (well-differentiated), grade 2 (moderately differentiated), and grade 3 (poorly differentiated). Necrotic areas constituting more than 10% of the tissue sections were regarded as 'extensive necrosis,' and the other cases were recorded as 'limited or no necrosis.' The presence of cancer cells within lymphovascular channels was reported as lymphovascular invasion.

Tissue microarray construction. Tissue microarray construction was performed as previously described (Kononen *et al*, 1998). Briefly, the haematoxylin and eosin-stained slides as well as the corresponding blocks were analysed by a pathologist. Representative areas of each case to be sampled were marked on the slides and blocks. Necrosis and extensive keratinisation areas were avoided. The specimen core selection from tissue blocks of the OSCCs included two 1.5-mm-diameter cores for each case. Because of the small specimens of verrucous hyperplasias and normal oral mucosas, only one 1.5-mm-diameter core for each case was selected. The selected cores were punched and transferred to paraffin-recipient blocks. Consecutive 4-μm-thick sections were produced, and haematoxylin and eosin staining was performed on each recipient block to confirm the presence of the selected zones.

Immunohistochemistry. Immunohistochemical stains were performed on 4-μm-thick sections from the tissue microarray by using the Leica Bond-Max autostainer (Leica Microsystems, Bondbiotech, Taichung, Taiwan) according to the manufacturer's instructions with minor modifications. Sections were deparaffinised using Bond Dewax Solution (Leica Microsystems) and rehydrated using graded alcohol. Heat-induced antigen retrieval was achieved using Bond Epitope Retrieval Solution 1 (Leica Microsystems) for 20 min at 100 °C. The slides were incubated in hydrogen peroxide for 5 min to reduce endogenous peroxidase activity. The slides were then incubated for 30 min at room temperature with mouse monoclonal antibodies against LC3B (1 : 50, clone 5F10, Nanotool, Teningen, Germany) and p62 (1 : 600, monoclonal, ab56416, Abcam, Cambridge, UK). Post-primary IgG linker reagent was applied for 8 min, and the slides were incubated with polymeric horseradish peroxidase IgG reagent for 8 min to localise the primary antibodies. Diaminobenzidine-tetrahydrochloride (DAB) was used as the substrate to detect antigen–antibody binding. Finally, haematoxylin was applied for 5 min to counterstain nuclei.

Evaluation of immunohistochemistry. The intensity, percentage, and sublocalisation of the immunohistochemical staining of each case were recorded. Nerve fibre and normal tonsillar tissue were used as positive controls for LC3B and p62, respectively. Staining omitting the primary antibody was performed as the negative control. The intensity and percentage of positively stained cells in each core were scanned at a low-powered field (× 100) and then evaluated at a high-powered field (× 400). LC3B staining was presented as cytoplasmic punctae (Ladoire *et al*, 2012). The intensity of LC3B punctae was recorded as: 0 to ⩽10 dots per cell, 1–11–20 dots per cell, 2 to >20 dots per cell without dot clusters, and 3 to >20 dots per cell with dot clusters. p62 staining was identified in the cytoplasm and nuclei. The intensity of p62 staining was recorded as 0, 1, 2, and 3 referring to negative, weak,

moderate, and strong staining, respectively. The percentage of positive cells of LC3B and p62 was recorded from 0 to 100%. The results of staining were scored using quick (Q) score, which was obtained by multiplying the percentage of positive cells (P) by the intensity (I) ($Q = P \times I$; maximum $= 300$; Charafe-Jauffret *et al*, 2004). The median values of the Q scores of OSCCs were used as cutoff points to classify cancer as exhibiting 'low expression' and 'high expression.'

RNA *in situ* hybridisation. *In situ* hybridisation was performed to examine the p62 mRNA by an RNAscope FFPE Assay Kit (Advanced Cell Diagnostics Inc., Hayward, CA, USA) and an RNAscope Probe Hs-p62/SQSTM1 (Advanced Cell Diagnostics Inc.) according to the manufacturer's instructions. Briefly, TMA sections were deparaffinised and pretreated with heat and protease, and then incubated with the probe targeting Hs-p62/SQSTM1 for 2 h at 40 °C. HeLa cell pallets were used as a positive control. Diaminobenzidine-tetrahydrochloride was used as the chromogen. Finally, haematoxylin was applied to counterstain the nuclei. Positive staining was identified as brown dots in the nucleus and/or cytoplasm.

The expression of p62 mRNA was evaluated by bright-field microscopy using the instructions in the RNAscope FFPE Assay Kit. We defined > 10 dots per cells in more than 10% of the tumour cells in one high-powered field ($\times 400$) as 'high expression'; the others were defined as 'low expression'.

Statistical analysis. Cronbach's α reliability analysis was used to quantify inter- and intraobserver variability of immunohistochemistry. The differences in p62 and LC3B expressions in normal oral mucosas, verrucous hyperplasias, and OSCCs were assessed using the Kruskal–Wallis test followed by Dunn's *post hoc* test. The correlations of p62 and LC3B expressions were evaluated using Spearman's correlation test and illustrated as scattered plots. The χ^2 test or Fisher's exact test was used to evaluate the association of categorical variables. Curves for overall survival and disease-specific survival were drawn using the Kaplan–Meier method, and the differences in survival rates were compared using log-rank tests. The univariate and multivariate Cox proportion regression models were used to estimate the hazard ratios and 95% confidence intervals for patients' outcomes. All *P*-values were two-sided. A *P*-value less than 0.05 was considered statistically significant. Statistical analysis was performed using SPSS Version 19.0 software (SPSS Inc., Armonk, NY, USA) for Windows.

RESULTS

Patient characteristics. A total of 195 OSCCs, 47 verrucous hyperplasias, and 37 normal oral mucosas were included in this study. The clinical information of all cases is summarised in Table 1. Among the 195 OSCC patients, 79 patients received postoperative adjuvant therapy: 60 patients treated with radiotherapy and chemotherapy, 16 patients treated with radiotherapy only, and 3 patients treated with chemotherapy only. The clinicopathologic characteristics of OSCC, including age, sex, tumour-node-metastasis stage, histologic grade, status of lymphovascular invasion, and necrosis, were presented in Table 2.

Inter- and intraobserver variability of immunohistochemistry. The immunohistochemical scoring for LC3B (cytoplasmic punctae) and p62 (cytoplasmic and nuclear) were examined for intra- and interobserver variabilities. Two pathologists independently evaluated the results of immunohistochemical staining without knowledge of clinicopathologic data. The interobserver agreement of the two pathologists was high ($\alpha = 0.977$ and $\alpha = 0.965$). The intraobserver agreement of the scoring also showed high

Table 1. Clinicopathologic characteristics of OSCCs, verrucous hyperplasias, and normal oral mucosas

	OSCC (n = 195)	Verrucous hyperplasia (n = 47)	Normal oral mucosa (n = 37)
Age (years)			
Mean ± s.d.	55.57 ± 11.97	52.21 ± 13.28	42.59 ± 14.67
Sex			
Male	187	44	25
Female	8	3	12
Tumour size (cm)			
Mean ± s.d.	3.00 ± 1.58	NA	NA

Abbreviations: NA = not analysed; OSCC = oral squamous cell carcinoma.

concordance ($\alpha = 0.935$). Conflicting results were resolved using a multiheaded microscope.

Comparison of LC3B expression in normal oral mucosas, verrucous hyperplasias, and OSCCs. All of the cases exhibited cytoplasmic LC3B punctae in various proportions of the cells (Figure 1A). The normal oral mucosas exhibited limited expression of LC3B punctae. Some verrucous hyperplasias exhibited focal increase in the number of LC3B punctae. The intensity of the punctae was sometimes heterogeneous in OSCCs, even in the same specimen. A proportion of the OSCCs presented a pattern similar to that of the normal oral muocsas, and certain cases exhibited dense clusters of dots. The median Q scores of LC3B were 5, 40, and 80 for the normal oral mucosas, verrucous hyperplasias, and OSCCs, respectively (Figure 1C). The differences in Q score between the three groups were statistically significant ($P < 0.001$).

Comparison of p62 protein expression in normal oral mucosas, verrucous hyperplasias, and OSCCs. Most of the normal oral mucosas exhibited moderate nuclear expression and weak cytoplasmic staining. The nuclear staining was predominantly located in the stratum spinosum of stratified squamous epithelia. The oral mucosas of verrucous hyperplasias exhibited variable nuclear and cytoplasmic expressions. We observed that the dysplastic cells at the stratum basale exhibited increased cytoplasmic expression and no nuclear expression. The OSCCs displayed various p62 expression patterns (Figure 1B). The medium Q scores of cytoplasmic p62 were 20, 60, and 100 for the normal oral mucosas, verrucous hyperplasias, and OSCCs, respectively (Figure 1C). Generally, the cytoplasmic expression in verrucous hyperplasias was stronger than that in normal oral mucosas ($P = 0.047$). The OSCCs exhibited the highest cytoplasmic p62 expression among the three groups ($P < 0.001$). Although diffuse loss of nuclear expression was observed in some OSCCs, the differences in nuclear expression between the three groups were statistically nonsignificant ($P = 0.067$; Figure 1C).

Correlation of LC3B and p62 protein expressions. We performed Spearman's correlation test to examine the relationships of LC3B and p62 expressions in normal oral mucosas, verrucous hyperplasias, and OSCCs (Figure 2). The relationship between cytoplasmic and nuclear expressions of p62 was modestly positively correlated in normal oral mucosas (rho $= 0.660$) and verrucous hyperplasias (rho $= 0.566$) but was negatively correlated in OSCCs (rho $= -0.347$). The relationship between LC3B and cytoplasmic p62 expression was positively correlated in OSCCs (rho $= 0.382$), verrucous hyperplasias (rho $= 0.439$), and normal

oral mucosas (rho = 0.370). The relationship between LC3B and nuclear p62 expressions exhibited weak to no correlation.

p62 mRNA expression in normal oral mucosas, verrucous hyperplasias, and OSCCs. The p62 mRNA expression detected using RNAscope showed no significant difference between normal oral mucosas, verrucous hyperplasias, and OSCCs ($P = 0.103$; Figure 3A and B). Most of the cases (240 out of 279, 86.02%) exhibited low p62 gene expression. In addition, high expression of p62 mRNA was associated with high expression of p62 protein in the cytoplasm ($P = 0.004$; Figure 3C).

Relationships between LC3B and p62 and clinicopathologic characteristics of OSCCs. The relationships between LC3B and p62 and clinicopathologic characteristics of OSCCs are summarised in Table 2. The median Q score of LC3B of the OSCCs was 80, which was used as a cutoff point. A total of 104 cases (53.33%) were classified as low expression, and 91 cases (46.67%) were

classified as high expression. High LC3B expression was associated with male and lymphovascular invasion.

The median Q scores of cytoplasmic and nuclear expressions of p62 were 100 and 140, respectively. Using the median score as a cutoff point, 103 cases (52.82%) were classified as low cytoplasmic expression, whereas 92 cases (47.18%) were classified as high cytoplasmic expression. High cytoplasmic expression of p62 was associated with positive lymph node status, advanced stage, high histologic grade, and lymphovascular invasion. The nuclear expression of 123 cases (63.08%) was subgrouped into low expression, and that of 72 cases (36.92%) was subgrouped into high expression. Low nuclear expression (Q score $\leqslant 140$) of p62 was related to high histologic grade.

Survival analysis. The mean follow-up time of OSCCs was 47.08 ± 32.37 months. The Kaplan–Meier survival analysis using log-rank tests indicated that low nuclear and high cytoplasmic p62 expressions were associated with poor overall and disease-specific

Table 2. Relationship between p62 and LC3B expression and clinicopathologic variables in OSCCs

Variable	No. of cases	p62 in cytoplasm			p62 in nucleus			LC3B		
		Low	High	*P*-value	Low	High	*P*-value	Low	High	*P*-value
Age										
$\leqslant$ 50 Years	71	38	33	0.882	41	30	0.243	39	32	0.735
> 50 Years	124	65	59		82	42		65	59	
Sex										
Male	187	97	90	0.285[a]	118	69	1.000[a]	97	90	0.001[a]*
Female	8	6	2		5	3		7	1	
T stage										
T1/T2	126	71	55	0.182	79	47	0.882	68	58	0.81
T3/T4	69	32	37		44	25		36	33	
N stage										
N0	145	86	59	0.002*	88	57	0.239	82	63	0.125
N1/N2/N3	50	17	33		35	15		22	28	
M stage										
M0	192	103	89	0.103[a]	120	72	0.298[a]	102	90	1.000[a]
M1	3	0	3		3	0		2	1	
Stage										
I/II	106	66	40	0.004*	63	43	0.25	60	46	0.318
III/IV	89	37	52		60	29		44	45	
Histologic grade										
G1/G2	168	101	67	<0.001*	101	67	0.033*	92	76	0.319
G3	27	2	25		22	5		12	15	
Lymphovascular invasion										
Absent	147	87	60	0.002*	90	57	0.348	85	62	0.028*
Present	48	16	32		33	15		19	29	
Necrosis										
Limited/no	145	86	59	0.002*	89	56	0.403	82	63	0.125
Extensive	50	17	33		34	16		22	28	

Abbreviation: OSCC = oral squamous cell carcinoma. *P<0.05.
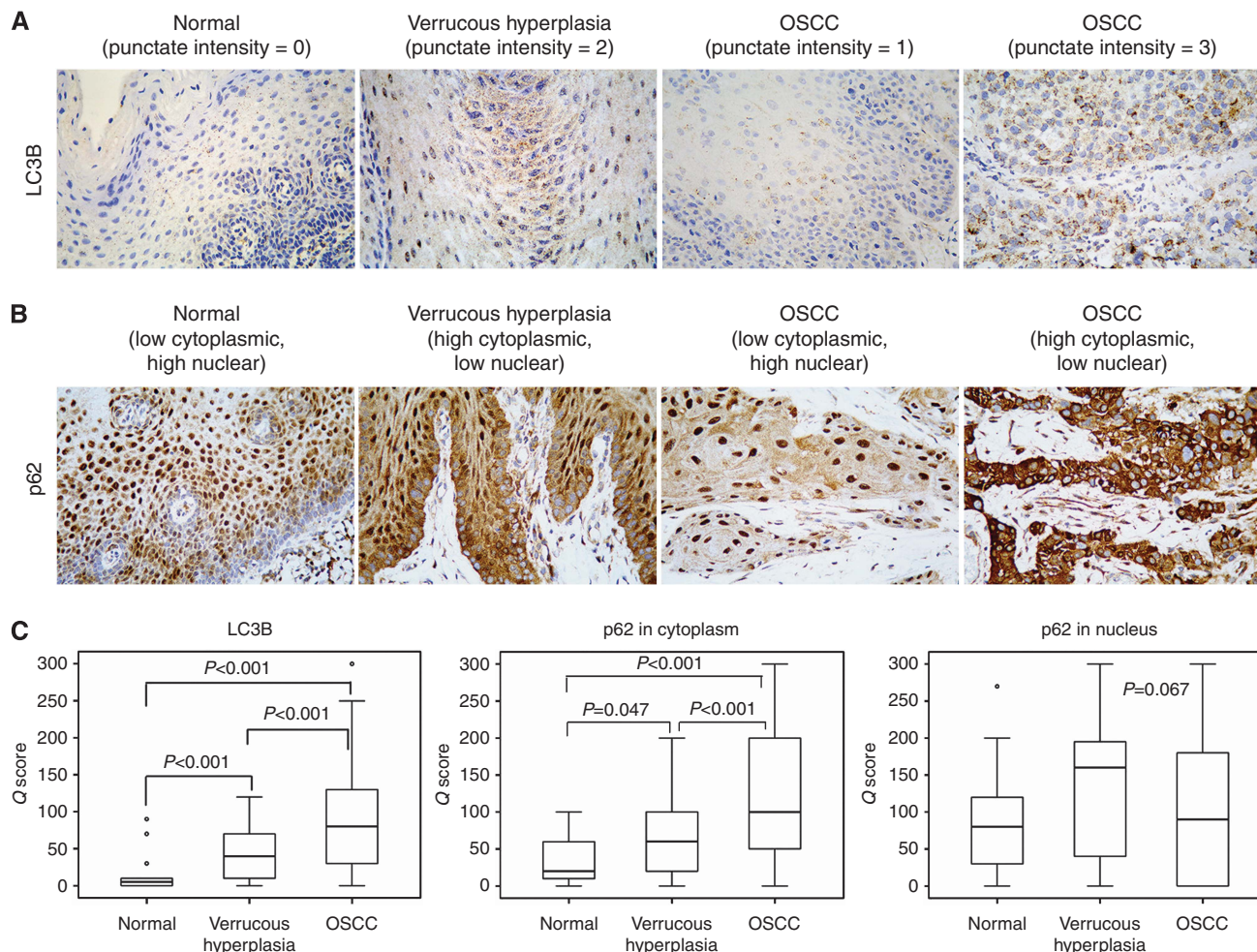[a]Fisher exact test.

Figure 1. The results of LC3B and p62 immunohistochemical stains in normal oral mucosas, verrucous hyperplasias, and OSCCs.
(**A**) Representative cases of LCB stainings (original magnification × 400). The normal oral mucosa shows limited LC3B punctae (intensity = 0). The verrucous hyperplasia exhibits focal increased in LC3 punctae (intensity = 2). The OSCCs show scanty LC3B punctae (intensity = 1) and marked increased LC3B punctae with dot clusters (intensity = 3). (**B**) Representative cases of p62 stainings (original magnification × 400). The normal oral mucosa exhibits low cytoplasmic and high nuclear p62 staining. The verrucous hyperplasia shows increased cytoplasmic p62 staining, and the dysplastic cells of basal layer shows negative nuclear staining. The OSCCs display various cytoplasmic and nuclear staining patterns. (**C**) Comparison of immunohistochemical Q scores of LC3B and p62 between OSCCs, verrucous hyperplasias, and normal oral mucosas. The medium lines of boxes show the median value, whereas top and bottom lines of boxes represent 75th and 25th percentiles, respectively. The ends of whiskers represent 10th and 90th percentiles. Open circles indicate the outliers.

survival rates. High LC3B expression was related to short disease-specific survival (Figure 4).

We further combined the immunoexpressions of the LC3B punctae (autophagosome marker) and cytoplasmic p62 (autophagy flux marker) to analyse the role of autophagy at early and advanced stages of OSCCs. According to their expression patterns, we classified the OSCCs into four groups: A, B, C, and D (Figure 5A). Group A (low LC3B and low p62) mimicked the basal level of autophagy in normal oral mucosas; Group B (low LC3B and high p62) represented a basal level of autophagy but impaired at late steps of the process; Group C (high LC3B and low p62) represented autophagy activation; and Group D (high LC3B and high p62) represented autophagy activation but impaired at late steps of the process. Regarding stage I and stage II OSCCs, no differences in overall survival ($P = 0.501$) and disease-specific survival ($P = 0.678$) were observed among the four groups. Regarding stage III and stage IV OSCCs, Groups B and D, which represented autophagy impairment under basal or activated autophagic activity, exhibited unfavourable overall survival and disease-specific survival compared with Groups A and C (Figure 5B).

Tables 3A–C show the results of the univariate and multivariate Cox proportional hazard analyses of clinicopathologic variables for overall survival, disease-specific survival, and recurrence-free survival, respectively. High LC3B and high cytoplasmic p62 were associated with unfavourable survival based on the univariate analysis. Low nuclear p62 expression was related to poor overall and disease-specific survival based on the univariate and multivariate analyses. Neither LC3B nor p62 was related to recurrence-free survival.

DISCUSSION

In this study, we first indicated that the protein expression of p62 and LC3B differed in normal oral mucosas, verrucous hyperplasias, and OSCCs. The results suggested that the autophagic activity was altered during carcinogenesis. Limited LC3B punctae and low cytoplasmic p62 expression in the normal oral mucosas of this study were consistent with the basal level of autophagy in normal cells. A recent research revealed that LC3B immunostaining was
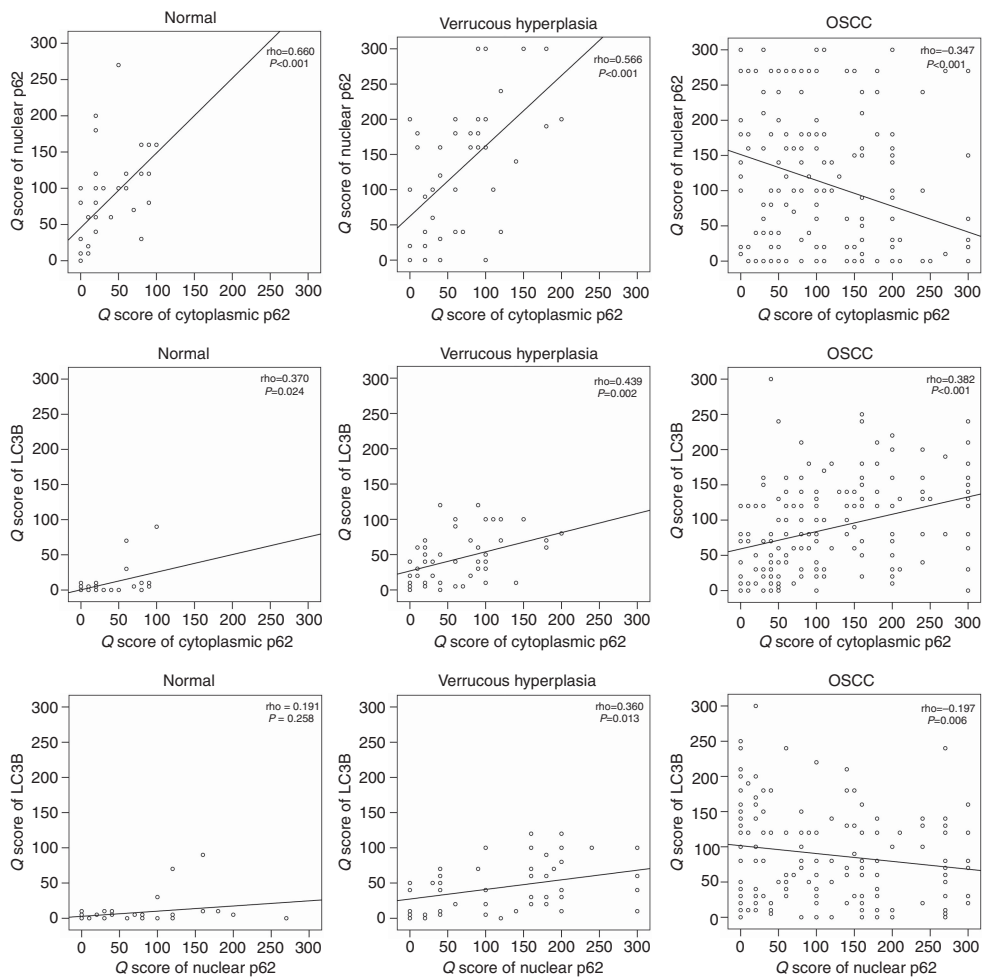
Figure 2. The relationships between p62 and LC3B protein expressions are illustrated as scattered plots with linear regression lines.
The relationship between cytoplasmic and nuclear expressions of p62 is modestly positively correlated in normal oral mucosas and verrucous hyperplasias but is negatively correlated in OSCCs. The relationship between LC3B and cytoplasmic p62 expression is positively correlated in all three groups. The relationship between LC3B and nuclear p62 expressions exhibits weak to no correlation.
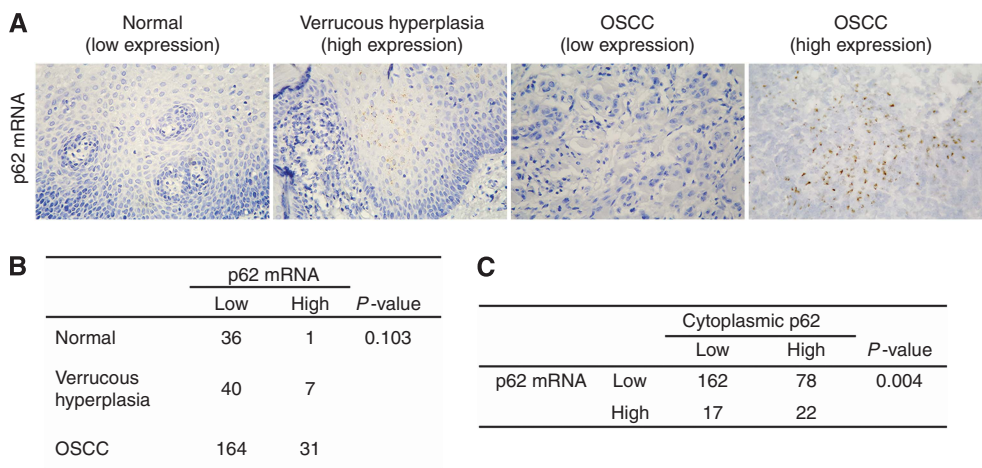

| | p62 mRNA | | |
	Low	High	P-value
Normal	36	1	0.103
Verrucous hyperplasia	40	7	
OSCC	164	31	

| | | Cytoplasmic p62 | | |
		Low	High	P-value
p62 mRNA	Low	162	78	0.004
	High	17	22	

Figure 3. The results of *in situ* hybridisation for p62 mRNA in normal oral mucosas, verrucous hyperplasias, and OSCCs. (**A**) Representative cases of p62 mRNA *in situ* hybridization (original magnification × 400). Most cases show limited to undetectable level of p62 mRNA. Some cases exhibit prominent p62 mRNA expression. (**B**) The difference of p62 mRNA expression in normal oral mucosas, verrucous hyperplasias, and OSCCs. It is not statistically significant ($P = 0.103$). (**C**) The relationship of p62 mRNA and protein expressions. High expression of mRNA is associated with high expression of protein in the cytoplasm.

elevated in most human cancer tissues compared with their normal counterparts (Ladoire *et al*, 2012). Our findings regarding oral tissue were similar to their results of other types of tissue. However, LC3B staining in the OSCCs can be heterogeneous even in the same specimen. We discovered that high expression of LC3B was associated with poor clinical outcomes of OSCCs.
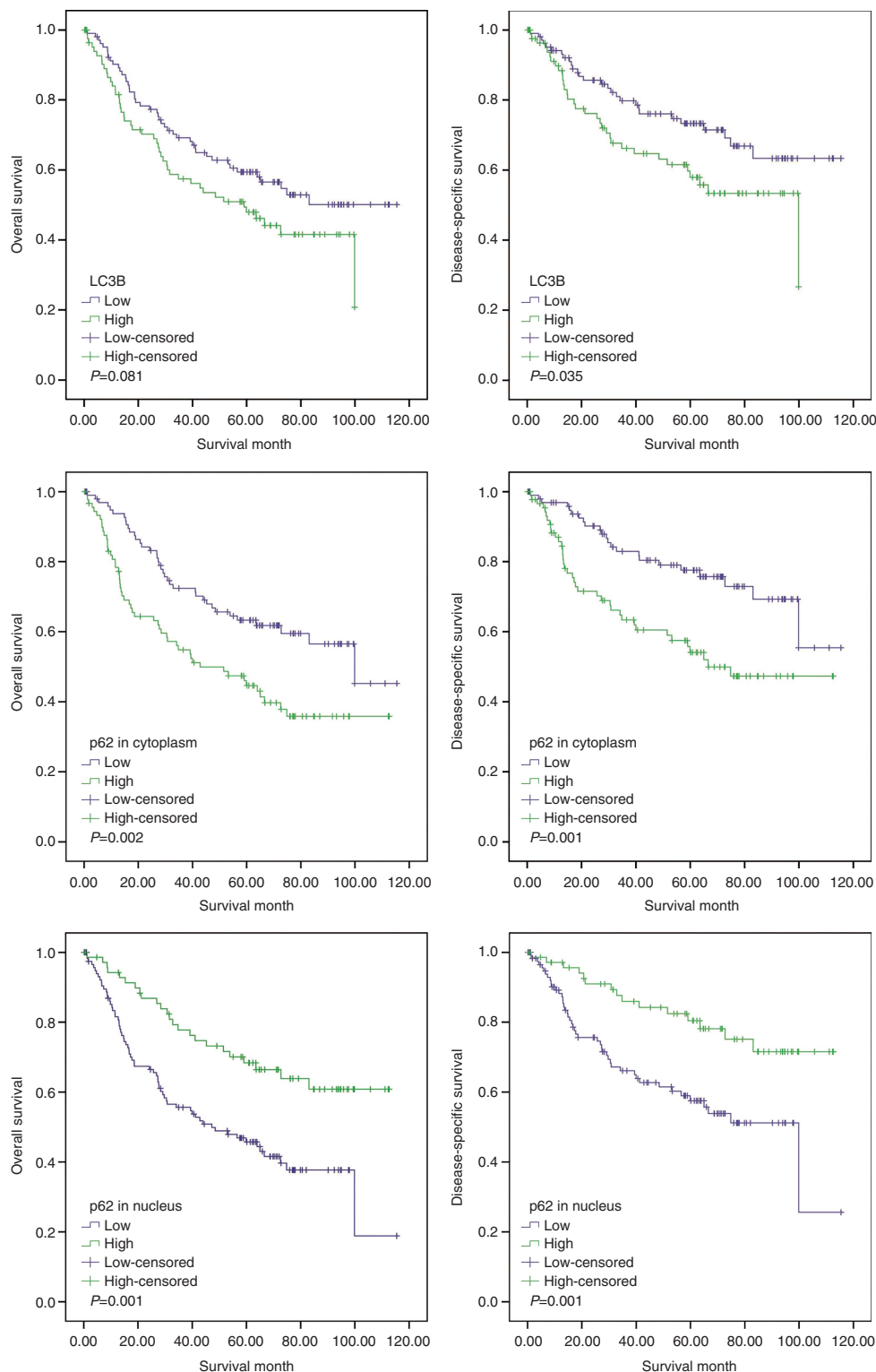
Figure 4. The Kaplan–Meier curves for overall survival and disease-specific survival rates according to LC3B and p62 expressions in OSCCs. High LC3B expression is related to short disease-specific survival. Low nuclear and high cytoplasmic p62 expressions are associated with poor overall and disease-specific survival rates.

During the process of autophagy, the soluble form LC3-I converts to lipidised form LC3-II, which associates with the membrane of autophagosomes. LC3 comprises three isoforms: LC3A, LC3B, and LC3C. The different functions of LC3 isoforms are not fully clarified. For example, LC3A and LC3B proteins may be increased under different stress conditions, and p62 degradation was involved in both pathways (Zois *et al*, 2011). Unlike definite

punctate pattern of LC3B, the immunohistochemical staining of LC3A recognized three distinct patterns: diffuse cytoplasmic, cytoplasmic/juxtanuclear, and 'stone-like' pattern (Sivridis *et al*, 2010). The results were not as straightforward as those of immunoblotting. Some authors claimed that maybe 'stone-like' pattern was associated with autophagy (Giatromanolaki *et al*, 2011b; Spowart *et al*, 2012). In fact, the biological meaning of
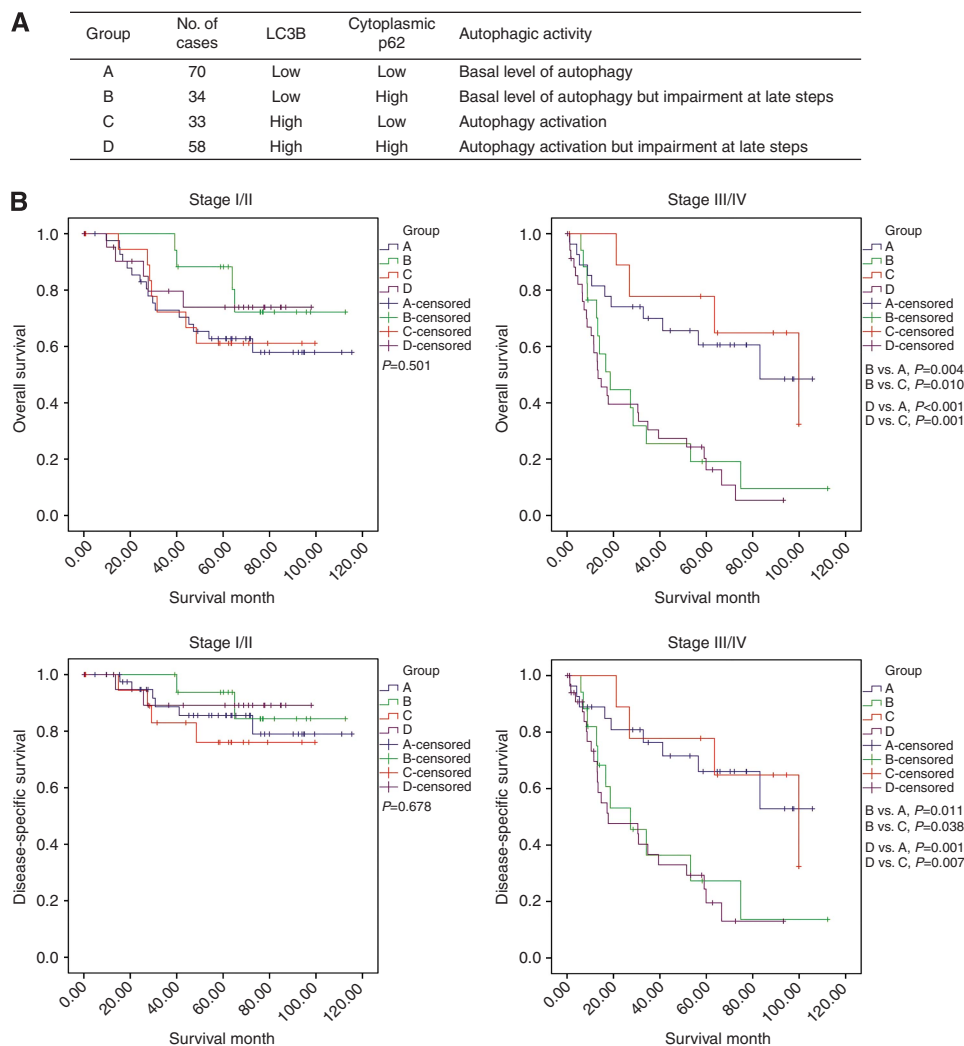
A

Group	No. of cases	LC3B	Cytoplasmic p62	Autophagic activity
A	70	Low	Low	Basal level of autophagy
B	34	Low	High	Basal level of autophagy but impairment at late steps
C	33	High	Low	Autophagy activation
D	58	High	High	Autophagy activation but impairment at late steps

B

Figure 5. Classification of OSCCs according to LC3B and cytoplasmic expression patterns. (**A**) Summary of the classification of the four groups: A, B, C, and D. (**B**) The Kaplan–Meier curves for overall survival and disease-specific survival rates of the four groups in OSCCs. No differences in overall survival and disease-specific survival are present among the four groups in stage I and stage II OSCCs. Groups B and D exhibit unfavourable overall survival and disease-specific survival compared with Groups A and C in stage III and stage IV OSCCs.

Table 3A. Univariate and multivariate Cox proportional hazard analyses of clinicopathologic variables for overall survival rate

Variable		Univariate analysis			Multivariate analysis		
		HR	95% CI	*P*-value	HR	95% CI	*P*-value
Age	>50 *vs* ⩽50 years	1.208	0.776–1.880	0.403	1.005	0.624–1.618	0.984
Sex	Male *vs* female	2.277	0.560–9.255	0.25	2.03	0.487–8.461	0.331
Stage	III/IV *vs* I/II	3.023	1.959–4.663	<0.001*	1.961	1.137–3.382	0.016*
Histologic grade	G3 *vs* G1/G2	1.37	0.760–2.470	0.295	0.91	0.453–1.828	0.792
Lymphovascular invasion	Present *vs* absent	3.507	2.277–5.400	<0.001*	2.187	1.290–3.709	0.004*
Necrosis	Extensive *vs* limited/no	1.782	1.153–2.755	0.009*	1.228	0.720–2.095	0.45
LC3B expression	High *vs* low	1.442	0.953–2.181	0.081	1.091	0.696–1.708	0.705
p62 cytoplasmic expression	High *vs* low	1.891	1.244–2.876	0.002*	1.441	0.900–2.305	0.128
p62 nuclear expression	Low *vs* high	2.243	1.402–3.589	0.001*	2.177	1.321–3.586	0.002*

Abbreviations: CI = confidence interval; HR = hazard ratio.

LC3A patterns has not been entirely elucidated. The expression of LC3C is much lower than that of LC3A and LC3B in all tissues (He *et al*, 2003). Thus, our study used LC3B immunohistochemical staining to identify autophagosome formation, although it inevitably missed the increase of other LC3 isoforms, which was a major limitation of our study.

Table 3B. Univariate and multivariate Cox proportional hazard analyses of clinicopathologic variables for disease-specific survival rate

Variable		HR	95% Confidence interval	P-value	HR	95% Confidence interval	P-value
		Univariate analysis			Multivariate analysis		
Age	>50 vs ≤50 years	1.095	0.645–1.857	0.738	0.876	0.487–1.574	0.657
Sex	Male vs female	3.04	0.421–21.953	0.27	2.077	0.276–15.610	0.478
Stage	III/IV vs I/II	5.624	3.090–10.237	<0.001*	4.105	2.034–8.287	<0.001*
Histologic grade	G3 vs G1/G2	1.415	0.696–2.877	0.338	1.115	0.479–2.598	0.801
Lymphovascular invasion	Present vs absent	4.641	2.780–7.748	<0.001*	2.119	1.177–3.818	0.012*
Necrosis	Extensive vs limited/no	1.651	0.967–2.820	0.066	0.884	0.457–1.709	0.714
LC3B expression	High vs low	1.711	1.033–2.833	0.035*	1.253	0.727–2.158	0.417
p62 cytoplasmic expression	High vs low	2.298	1.368–3.862	0.001*	1.736	0.980–3.076	0.059
p62 nuclear expression	Low vs high	2.545	1.414–4.579	0.002*	2.571	1.356–4.874	0.004*

Abbreviation: HR = hazard ratio

Table 3C. Univariate and multivariate Cox proportional hazard analyses of clinicopathologic variables for recurrence-free survival rate

Variable		HR	95% Confidence interval	P-value	HR	95% Confidence interval	P-value
		Univariate analysis			Multivariate analysis		
Age	>50 vs ≤50 years	0.845	0.500–1.427	0.528	0.817	0.470–1.420	0.473
Sex	Male vs female	1.057	0.330–3.384	0.925	1.151	0.349–3.799	0.818
Stage	III/IV vs I/II	1.711	1.024–2.859	0.040*	1.025	0.506–2.078	0.945
Histologic grade	G3 vs G1/G2	0.852	0.365–1.985	0.704	0.835	0.306–2.279	0.725
Lymphovascular invasion	Present vs absent	2.692	1.533–4.727	<0.001*	2.661	1.269–5.583	0.010*
Necrosis	Extensive vs limited/no	1.163	0.655–2.068	0.606	1.238	0.616–2.489	0.549
LC3B expression	High vs low	0.886	0.521–1.507	0.654	0.889	0.508–1.557	0.681
p62 cytoplasmic expression	High vs low	0.802	0.475–1.354	0.408	0.745	0.415–1.338	0.324
p62 nuclear expression	Low vs high	1.142	0.675–1.934	0.619	1.249	0.722–2.163	0.427

Abbreviation: HR = hazard ratio *P<0.05.

A reliable method to detect the dynamic process of autophagy in clinical specimens is unavailable. Immunohistochemistry is the most common method used to analyse autophagy in formalin-fixed, paraffin-embedded tissues. Using high-quality LC3B antibody clone 5F10 achieves maximal sensitivity to detect autophagosome formation (Ladoire *et al*, 2012; Martinet *et al*, 2013). Remarkably, the increase in LC3 punctae, which indicates an increased number of autophagosomes, represents activation of autophagy or suppression of steps after autophagosome formation. Thus, using LC3B staining alone without simultaneously monitoring the autophagy flux to analyse the autophagy activity of OSCCs in a previous study could be problematic (Tang *et al*, 2013).

p62, as a substrate of autophagy, is widely used as a marker to monitor autophagic flux (Mizushima *et al*, 2010). The p62 protein expression was controlled by transcriptional regulation and by post-transcriptional autophagic degradation (Puissant *et al*, 2012). Our results showed that the level of p62 mRNA is similar in normal oral mucosas, verrucous hyperplasias, and OSCCs, and the transcription was activated in a minority of cases. However, p62 could induct positive feedback loops to stimulate its own transcription (Jain *et al*, 2010; Ling *et al*, 2012). Under certain conditions, autophagy impairment, which leads to accumulation of p62 protein, may also increase the level of p62 mRNA. Therefore, in most of cases, increased p62 protein indicates the impairment of autophagy. We determined that increased expression of cytoplasmic p62 protein was associated with poor prognosis, which was similar to a finding of a recent study (Inui *et al*, 2013). In the present study, we further classified the OSCCs into four groups according to the expression patterns of cytoplasmic p62 and LC3B. Our results indicated that high p62 cytoplasmic expression, regardless of LC3B expression, was associated with unfavourable outcomes in advanced OSCCs. The results suggested that autophagy impairment, at either early or late steps of the process, contributes to tumour progression and is associated with unfavourable clinical outcomes in advanced OSCCs. We also observed that early-stage tumours (stages I and II) with functional autophagy, either under a basal or activated condition (Groups A and C), tend to exhibit poor overall survival, compared with tumours with impaired autophagy (Groups B and D); however, the difference was statistically nonsignificant. This observation suggested that functional autophagy might promote tumour progression during the early carcinogenesis. Thus, autophagy may have distinct roles at early and late stages of cancer. Additional studies

should be performed to clarify the relationship between autophagy and carcinogenesis in OSCCs.

The function of p62 in the nucleus is largely unknown. We discovered that the nuclear p62 expression primarily occurred on differentiated layers, particularly on the stratum spinosum. The dysplastic cells of verrucous hyperplasias exhibited high cytoplasmic expression but no nuclear expression. In addition, loss of nuclear expression was related to high histologic grade of the OSCCs. All of the findings indicate that p62 might have a role in cell differentiation.

Compared with normal oral mucosas and verrucous hyperplasias, the OSCCs exhibited tendencies of loss of nuclear expression and increase in the cytoplasmic accumulation of p62. These characteristics were also associated with poor prognostic factors and poor survival status. Recent studies have stated that the increased cytoplasmic accumulation of p62 was located in neoplastic tissue and linked to poor prognosis of various types of cancers (Kitamura et al, 2006; Inoue et al, 2012; Inui et al, 2013; Luo et al, 2013; Ren et al, 2014). However, the association of the subcellular localisation of p62 with carcinogenesis has rarely been mentioned. We first indicated that nuclear p62 expression was an independent prognostic factor of OSCCs. p62 is a nucleocytoplasmic shuttling protein and can be found in nuclear promyelocytic leukaemia bodies (Pankiv et al, 2010). Our data indicated that the cytoplasmic and nuclear expressions of p62 were positively correlated in the normal oral mucosas and verrucous hyperplasias but were negatively correlated in the OSCCs. These findings imply that the nucleocytoplasmic shuttling of p62 might be altered in cancers, and the phenomenon may relate to carcinogenesis.

Another limit of our study was relatively small sample size of verrucous hyperplasia, a precursor lesion to OSCC. The surgical resected specimens of verrucous hyperplasia were generally small for tissue microarray construction. The small specimens usually displayed areas of cauterised artefact, which cause difficulty to interpretate in immunohistochemical studies. In the limited number of verrucous hyperplasias, we disclosed that their expression patterns of LC3B and p62 were between normal oral mucosas and OSCCs. Larger studies regarding the relationships of autophagy and progression of verrucous hyperplasia are necessary.

In conclusion, we examined the different expression patterns of LC3B and p62 in normal oral mucosas, verrucous hyperplasias, and OSCCs. High LC3B expression and altered p62 subcellular localisation were associated with aggressive clinicopathologic features and poor prognosis of OSCCs. The results of this study implied that autophagy impairment contributed to cancer progression in the OSCCs.

ACKNOWLEDGEMENTS

CONFLICT OF INTEREST

The authors declare no conflict of interest.

REFERENCES

Brech A, Ahlquist T, Lothe RA, Stenmark H (2009) Autophagy in tumour suppression and promotion. *Mol Oncol* **3**(4): 366–375.

Charafe-Jauffret E, Tarpin C, Bardou VJ, Bertucci F, Ginestier C, Braud AC, Puig B, Geneix J, Hassoun J, Birnbaum D (2004) Immunophenotypic analysis of inflammatory breast cancers: identification of an 'inflammatory signature'. *J Pathol* **202**(3): 265–273.

Choi J, Jung W, Koo JS (2013) Expression of autophagy-related markers beclin-1, light chain 3A, light chain 3B and p62 according to the molecular subtype of breast cancer. *Histopathology* **62**(2): 275–286.

Giatromanolaki A, Koukourakis MI, Koutsopoulos A, Chloropoulou P, Liberis V, Sivridis E (2011a) High Beclin 1 expression defines a poor prognosis in endometrial adenocarcinomas. *Gynecol Oncol* **123**(1): 147–151.

Giatromanolaki AN, Charitoudis GS, Bechrakis NE, Kozobolis VP, Koukourakis MI, Foerster MH, Sivridis EL (2011b) Autophagy patterns and prognosis in uveal melanomas. *Mod Pathol* **24**(8): 1036–1045.

He H, Dang Y, Dai F, Guo Z, Wu J, She X, Pei Y, Chen Y, Ling W, Wu C (2003) Post-translational modifications of three members of the human MAP1LC3 family and detection of a novel type of modification for MAP1LC3B. *J Biol Chem* **278**(31): 29278–29287.

Huang JJ, Li HR, Huang Y, Jiang WQ, Xu RH, Huang HQ, Lv Y, Xia ZJ, Zhu XF, Lin TY, Li ZM (2010) Beclin 1 expression: a predictor of prognosis in patients with extranodal natural killer T-cell lymphoma, nasal type. *Autophagy* **6**(6): 777–783.

Inoue D, Suzuki T, Mitsuishi Y, Miki Y, Suzuki S, Sugawara S, Watanabe M, Sakurada A, Endo C, Uruno A, Sasano H, Nakagawa T, Satoh K, Tanaka N, Kubo H, Motohashi H, Yamamoto M (2012) Accumulation of p62/SQSTM1 is associated with poor prognosis in patients with lung adenocarcinoma. *Cancer Sci* **103**(4): 760–766.

Inui T, Chano T, Takikita-Suzuki M, Nishikawa M, Yamamoto G, Okabe H (2013) Association of p62/SQSTM1 excess and oral carcinogenesis. *PLoS One* **8**(9): e74398.

Jain A, Lamark T, Sjøttem E, Larsen KB, Awuh JA, Øvervatn A, McMahon M, Hayes JD, Johansen T (2010) p62/SQSTM1 is a target gene for transcription factor NRF2 and creates a positive feedback loop by inducing antioxidant response element-driven gene transcription. *J Biol Chem* **285**(29): 22576–22591.

Kapoor V, Paliwal D, Baskar Singh S, Mohanti BK, Das SN (2012) Deregulation of Beclin 1 in patients with tobacco-related oral squamous cell carcinoma. *Biochem Biophys Res Commun* **422**(4): 764–769.

Kitamura H, Torigoe T, Asanuma H, Hisasue SI, Suzuki K, Tsukamoto T, Satoh M, Sato N (2006) Cytosolic overexpression of p62 sequestosome 1 in neoplastic prostate tissue. *Histopathology* **48**(2): 157–161.

Kononen J, Bubendorf L, Kallioniemi A, Barlund M, Schraml P, Leighton S, Torhorst J, Mihatsch MJ, Sauter G, Kallioniemi OP (1998) Tissue microarrays for high-throughput molecular profiling of tumor specimens. *Nat Med* **4**(7): 844–847.

Koukourakis MI, Giatromanolaki A, Sivridis E, Pitiakoudis M, Gatter KC, Harris AL (2010) Beclin 1 over- and underexpression in colorectal cancer: distinct patterns relate to prognosis and tumour hypoxia. *Br J Cancer* **103**(8): 1209–1214.

Kundu M, Thompson CB (2008) Autophagy: basic principles and relevance to disease. *Annu Rev Pathol* **3**: 427–455.

Ladoire S, Chaba K, Martins I, Sukkurwala AQ, Adjemian S, Michaud M, Poirier-Colame V, Andreiuolo F, Galluzzi L, White E, Rosenfeldt M, Ryan KM, Zitvogel L, Kroemer G (2012) Immunohistochemical detection of cytoplasmic LC3 puncta in human cancer specimens. *Autophagy* **8**(8): 1175–1184.

Levine B (2007) Cell biology: autophagy and cancer. *Nature* **446**(7137): 745–747.

Levine B, Kroemer G (2008) Autophagy in the pathogenesis of disease. *Cell* **132**(1): 27–42.

Ling J, Ya Kang, Zhao R, Xia Q, Lee D-F, Chang Z, Li J, Peng B, Fleming JB, Wang H (2012) Kras^{G12D}-induced IKK2/β/NF-κB activation by IL-1α and p62 feedforward loops is required for development of pancreatic ductal adenocarcinoma. *Cancer Cell* **21**(1): 105–120.

Luo RZ, Yuan ZY, Li M, Xi SY, Fu J, He J (2013) Accumulation of p62 is associated with poor prognosis in patients with triple-negative breast cancer. *OncoTargets Ther* **6**: 883–888.

Martinet W, Schrijvers DM, Timmermans JP, Bult H, De Meyer GR (2013) Immunohistochemical analysis of macroautophagy: recommendations and limitations. *Autophagy* **9**(3): 386–402.

Mizushima N (2007) Autophagy: process and function. *Genes Dev* **21**(22): 2861–2873.

Mizushima N, Levine B, Cuervo AM, Klionsky DJ (2008) Autophagy fights disease through cellular self-digestion. *Nature* **451**(7182): 1069–1075.

Mizushima N, Yoshimori T, Levine B (2010) Methods in mammalian autophagy research. *Cell* **140**(3): 313–326.

Nicotra G, Mercalli F, Peracchio C, Castino R, Follo C, Valente G, Isidoro C (2010) Autophagy-active beclin-1 correlates with favourable clinical outcome in non-Hodgkin lymphomas. *Mod Pathol* **23**(7): 937–950.

Pankiv S, Lamark T, Bruun JA, Overvatn A, Bjorkoy G, Johansen T (2010) Nucleocytoplasmic shuttling of p62/SQSTM1 and its role in recruitment of nuclear polyubiquitinated proteins to promyelocytic leukemia bodies. *J Biol Chem* **285**(8): 5941–5953.

Puissant A, Fenouille N, Auberger P (2012) When autophagy meets cancer through p62/SQSTM1. *Am J Cancer Res* **2**(4): 397.

Qu X, Yu J, Bhagat G, Furuya N, Hibshoosh H, Troxel A, Rosen J, Eskelinen EL, Mizushima N, Ohsumi Y, Cattoretti G, Levine B (2003) Promotion of tumorigenesis by heterozygous disruption of the beclin 1 autophagy gene. *J Clin Invest* **112**(12): 1809–1820.

Ren F, Shu G, Liu G, Liu D, Zhou J, Yuan L, Zhou J (2014) Knockdown of p62/sequestosome 1 attenuates autophagy and inhibits colorectal cancer cell growth. *Mol Cell Biochem* **385**(1–2): 95–102.

Shintani T, Klionsky DJ (2004) Autophagy in health and disease: a double-edged sword. *Science* **306**(5698): 990–995.

Sivridis E, Koukourakis MI, Zois CE, Ledaki I, Ferguson DJ, Harris AL, Gatter KC, Giatromanolaki A (2010) LC3A-positive light microscopy detected patterns of autophagy and prognosis in operable breast carcinomas. *Am J Pathol* **176**(5): 2477–2489.

Spowart JE, Townsend KN, Huwait H, Eshragh S, West NR, Ries JN, Kalloger S, Anglesio M, Gorski SM, Watson PH, Gilks CB, Huntsman DG, Lum JJ (2012) The autophagy protein LC3A correlates with hypoxia and is a prognostic marker of patient survival in clear cell ovarian cancer. *J Pathol* **228**: 437–447.

Tang JY, Hsi E, Huang YC, Hsu NC, Chu PY, Chai CY (2013) High LC3 expression correlates with poor survival in patients with oral squamous cell carcinoma. *Hum Pathol* **44**(11): 2558–2562.

Wan XB, Fan XJ, Chen MY, Xiang J, Huang PY, Guo L, Wu XY, Xu J, Long ZJ, Zhao Y (2010) Elevated Beclin 1 expression is correlated with HIF-1alpha in predicting poor prognosis of nasopharyngeal carcinoma. *Autophagy* **6**(3): 395–404.

Wang Y, Wang C, Tang H, Wang M, Weng J, Liu X, Zhang R, Huang H, Hou J (2013) Decrease of autophagy activity promotes malignant progression of tongue squamous cell carcinoma. *J Oral Pathol Med* **42**(7): 557–564.

Warnakulasuriya S (2009) Global epidemiology of oral and oropharyngeal cancer. *Oral Oncol* **45**(4–5): 309–316.

Won KY, Kim GY, Lim SJ, Kim YW (2012) Decreased Beclin-1 expression is correlated with the growth of the primary tumor in patients with squamous cell carcinoma and adenocarcinoma of the lung. *Hum Pathol* **43**(1): 62–68.

Yue Z, Jin S, Yang C, Levine AJ, Heintz N (2003) Beclin 1, an autophagy gene essential for early embryonic development, is a haploinsufficient tumor suppressor. *Proc Natl Acad Sci USA* **100**(25): 15077–15082.

Zois CE, Giatromanolaki A, Sivridis E, Papaiakovou M, Kainulainen H, Koukourakis MI (2011) "Autophagic flux" in normal mouse tissues: focus on endogenous LC3A processing. *Autophagy* **7**(11): 1371–1378.